

Judit Schneider · Tamás Tél

Extracting flow structures from tracer data

Received: 29 October 2002 / Accepted: 7 February 2003
© Springer-Verlag 2003

Abstract A method of visualizing structures in closed chaotic flows out of homogenous particle distributions is presented in the example of models of a meandering jet. To this end, the system will be leaked or opened up by defining a region of the flow, so that a particle is considered to be escaped if it leaves this region. By applying this method to an ensemble of nonescaped tracers, we are able to characterize mixing processes by visualizing the converging and stretching filamentations (stable and unstable manifolds) in the flow without using additional mathematical tools. The possibility of applying the algorithm to analyze buoy data, and a comparison with the finite time manifolds are discussed.

Keywords Meandering jet · Chaos · Filamentation · Stable and unstable manifolds

1 Introduction

Chaotic advection and the related mixing processes in environmental flows have been widely studied in recent years (Huppert et al. 1998; Ottino 1989; Farmer et al. 2002; Perugini et al. 2002). Advection in the Gulf Stream has attracted special attention since mixing there can change important features such as temperature and salinity distributions (Flagg et al. 2002), or it can affect distributions of nutrients (Alperin et al. 2002) or of pollutants such as oil (deFatima et al. 2002). To describe the basic dynamics of the Gulf Stream, Bower proposed a two-dimensional kinematic model (Bower 1991), since

the Stream appears two-dimensional along isopycnal surfaces. Samelson (1992) (see also Cencini et al. 1999) introduced time dependence in this model to simulate mixing processes. Dutkiewicz and Paldor (1994) enhanced mixing via the interaction with a spatially fixed eddy which perturbs the velocity field of the meander. del Castillo-Negrete and Morisson (1994) (see also Rogerson et al. 1999; Yuan et al. 2002) replaced the models by a dynamically consistent one, compatible with the quasigeostrophic equation, where chaotic advection is due to Rossby waves in the Bickley jet. The basic dynamical mechanism responsible for chaos is in all the models the nontrivial time dependence of the velocity field, which alone is sufficient to convert advection to be chaotic (Ott 1993).

It is worth mentioning that, in spite of the barotropic nature of these models, variations in their parameters parametrize changes in the depth of the oceanic jet (see Yuan et al. 2002); the models therefore reflect certain baroclinic effects also.

Mixing, or Lagrangian dynamics in general, can be made visible by tracer particles, which will be treated as point-like particles with the same density as the surrounding fluid (Knobloch and Weiss 1987). Such tracers could be, for example, plankton or chemical substances (for reactive flows see Toroczka and Tél 2002) or buoys. In environmental flows, chaotic mixing generates filamental structures which give information about the underlying dynamics. Gradients of the temperature field (SST) and of the potential vorticity can be used to detect these filaments.

In experiments, a simple method to obtain structures out of closed flows without any biological or chemical reactions is to add dye particles (Rothstein et al. 1999; Voth et al. 2002). In closed flows (flows in closed basins) which are sufficiently chaotic, idealized tracer particles will trace out structures of the flow for a short period, but after a certain transient time, they will be distributed homogeneously. The advection dynamics is area- or volume-preserving due to the incompressibility of the flow, and the asymptotic dis-

Responsible Editor: Jörg-Olaf Wolff

J. Schneider (✉)
Department for Physics, University of Potsdam,
PF 601553, 14415 Potsdam, Germany
e-mail: jotes@lenne.agnld.uni-potsdam.de

T. Tél
Institute for Theoretical Physics, Eötvös University,
Pf. 32, H-1538, Budapest, Hungary

tribution in such systems is uniform over the chaotic region (Ott 1993).

The question which arises here is whether it is possible to obtain again some structure out of this homogenous distribution of particles in closed flows. Can we extract some information from this state about the complicated Lagrangian dynamics of the system, which is completely described in the Eulerian sense by the set of smooth streamlines? Here, we propose the method of leaking (Schneider et al. 2002), which is shown to provide a kind of fingerprint of the closed system's advection dynamics.

2 Visualizing Lagrangian filamentation

The method we propose is based on chaos theory (Tél 1990; Lai et al. 1993; Ott 1993) and its novelty lies in its application to a hydrodynamical problem. The idea is to make Lagrangian, i.e., tracer-related structures, visible, which have definite dynamical meanings: lines of intense stretching and lines of convergence. In the language of dynamical system theory, these lines are tangent to the eigenvectors corresponding to the positive and negative Lyapunov exponents of the tracer dynamics, and provide the unstable and the stable foliation, respectively (Alvarez et al. 1998; Giona et al. 1999). These lines are present in any flow generating chaotic advection, but in closed flows both types of them are fully space-filling, and hence do not appear as clearly visible spatial structures.

To visualize the Lagrangian filamentation, we propose to consider a finite preselected region obtained by subtracting the leaked region from the full closed flow, and specify trajectories out of an ensemble of tracers which do not leave this region in a time interval ($t_0 < t < t_0 + \tau$), where t_0 is an arbitrary initial moment and τ is a time span definitely longer than the natural time scale of the flow (Schneider et al. 2002). The initial ($t = t_0$) positions of these trajectories define the location of long lifetimes in the preselected region, and hence the direction of converging motion (Lai et al. 1993) (see the schematic Fig. 1). The final ($t = t_0 + \tau$) positions of the same trajectories fall on curves along which trajectories are about to escape the preselected region. Their tangents correspond to the local stretching directions (Lai et al. 1993). The midpoints ($t = t_0 + \tau/2$) of the trajectories must be close to tracer positions which never escape the region.

In terms of chaos theory, the set from which particles never escape the system (both forward and backward in time) is called the chaotic saddle. It consists of an infinite number of hyperbolic points, each of them possessing a stable and an unstable manifold. The stable manifold (converging filament in Fig. 1) is the set of initial points from which the given hyperbolic point can be reached. The unstable manifold (stretching filament in Fig. 1) is the curve along which points from a close neighborhood of the hyperbolic points leave the point. Stable and

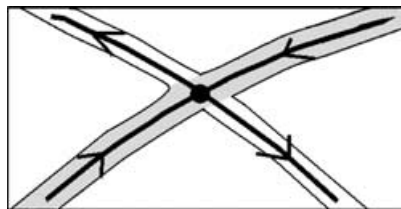


Fig. 1 Filamentations due to a never-escaping (hyperbolic) orbit of the advection dynamics. A trajectory can stay over a long time τ in a preselected region (*rectangle*) of the flow, if its initial ($t = t_0$) position is in a narrow slab (*gray region*) around a line (the converging filament) which leads to the never-escaping orbit (*black dot*). The endpoint ($t = t_0 + \tau$) of this trajectory is then necessarily in a narrow slab (*white region*) around another curve (the stretching filament) along which particles flow away from the never-escaping orbit (after an infinitely long time). The midpoint ($t = t_0 + \tau/2$) of the trajectory must then be in any case around the never-escaping orbit itself. For better visualization, the bands are magnified. Their real width is an exponentially decreasing function of the time span τ , and after a few flow periods, the bands typically become narrower than the width provided by the plotting device. In chaotic flows the situation is much more complicated than the one shown here, since there is an infinity of never-escaping orbits which form a fractal, and hence both the converging/stable and stretching/unstable filamentations are fractal objects

unstable manifolds and the chaotic saddle itself possess fractal dimensions (Tél 1990).

A good guess at an appropriate value of τ is the average lifetime of chaos in the leaked flow. Although this might also depend on the precise form and location of the leak (for a discussion see Schneider et al. 2002), a typical estimate is $-1/\ln(1 - \Delta)$, with Δ as the area of the leak divided by the area of the unleaked chaotic flow. In particular, for small leaks the lifetime is approximately $1/\Delta$.

In strictly time-periodic flows the chaotic saddle and its manifolds change with the period of the flow but are invariant on a stroboscopic picture taken with the period. In flows with nonperiodic (quasiperiodic or chaotic) time dependence and with smooth space dependence of the velocity field, recent theories (Jacobs et al. 1997; Neufeld and Tél 1998) predict that the same objects remain well defined (although not invariant on any snapshot) and their fractal dimension is independent of the time (t_0 and τ) of observation (provided the latter is sufficiently long).

In any case, the actual shape (and dimension) of these objects depend on the choice of the considered region (the choice of the leak), but any filament of them is an exact part of the closed system's filamentation. Thus, by selecting larger and larger regions (smaller and smaller leaks), a convergence towards full filamentation can be seen. So, for any sufficiently large region, a faithful approximant of the closed system's stretching and converging directions can be obtained. These filaments clearly define the stretching and converging directions around a given point of the leaked flow, but the same direction characterizes also the closed flow at the same point.

3 Models and results

3.1 Time-periodic kinematic model

The model of Bower (1991) and Samelson (1992) describes a meandering jet flowing eastward (to the right) whose velocity field is described in a frame comoving with the jet:

$$\Psi(x, y, t) = \Psi_0 \left[1 - \tanh \frac{y - A \cos(kx)}{\lambda \sqrt{1 + k^2 A^2 \sin^2(kx)}} \right] + cy. \quad (1)$$

Here, A is the amplitude, λ sets the jet's width, k stands for the wavenumber, and c is the phase speed. We handle this model as a closed flow, by imposing periodic boundary conditions in x . The velocity is highest in the middle of the stream (jet) and decreases towards the edges (corresponding to the decreasing density of the streamlines). Idealized tracer particles, which are point-like and adopt the velocity of the fluid at once, follow exactly the instantaneous streamlines. In the comoving frame used, the stream is clearly divided into three regions: a central jet flowing to the right, an outer flow of small negative average velocity, and closed recirculation cells at the edges (see Fig. 2a).

The tracer's equations of motion can be derived from the streamfunction:

$$\dot{y} = v_y = \frac{\partial \Psi}{\partial x}, \quad \dot{x} = v_x = -\frac{\partial \Psi}{\partial y}. \quad (2)$$

Introducing a simple time dependence, e.g., varying the amplitude of the streamfunction periodically in time with the period $T = 2\pi/\omega$:

$$A = A_0 [1 + \sigma \cos(\omega t + \theta)], \quad (3)$$

where ω is the perturbation frequency, σ the perturbation amplitude, and θ a constant phase shift; tracer particles do not move along the streamlines. This perturbation corresponds to a periodic change of the amplitude/width of the Gulf Stream (Samelson 1992).

For a perturbation amplitude of $\sigma = 0.3$ ($\omega = 0.4$, $\theta = \pi/2$), the motion of tracer particles is already highly chaotic. With the dimensionless parameters used, models (1) and (3) correspond to a jet of width 40 km, speed 1 m s^{-1} , wavelength 260 km, and perturbation period of 8 days (see Cencini et al. 1999). The chaotic regime lies between the lines $|y| < y_0$, where $y_0 = 3.5$. After long times, particles can move freely within the whole width of the stream; no region of the flow is preferred. This can be demonstrated by monitoring the motion of a droplet in the chaotic flow (Fig. 2). Starting a droplet of dye consisting of $N = 10\,000$ particles, the droplet will be deformed: it will be stretched and folded, as is characteristic for chaotic motion. Asymptotically, all particles are distributed homogeneously in the whole stream. Can some local information be extracted from the homogeneous state?

To this end we apply the method of leaking described in the previous section: two lines will be defined inside the stream, parallel to the mean flow direction, for example at $y = y_c = 2.7$ and $y = -y_c$ (for keeping the symmetry of the stream). Particles which cross these borders outwards will be treated as escaped, and are taken out of the flow. Thus, the borders serve as a kind of semipermeable walls which allow only the particles to leave the stream. In this way, the formerly closed system is opened up by leaking, and escape of particles is possible.

Starting from a homogenous particle distribution, particles which have not yet escaped over a certain time will trace out filamental structures (see Fig. 3) if we analyze these trajectories as described in Section 2. Comparing the traced-out structures with the streamlines of the unperturbed flow (Fig. 2a) shows that they still hold some similarity, even if the motion of particles is highly chaotic: the central jet is clearly visible and the structures on the edges somewhat resemble the recirculation cells.

The traced-out structures are not only filamental but also have a fixed fractal dimension of less than 2. Varying the width of the leak results in a change of the fractal dimension: if the area of the leaks increases, i.e., if $y_0 - y_c$ increases, the fractal dimension of the system decreases. Thus, the traced-out structures are more rarified. On the other hand, by decreasing the width of the leaks towards zero ($y_c \rightarrow y_0$), more particles remain in the system and their traced-out structures fatten and become denser. They reach a dimension of $d = 2$ for a leak of zero area, and the filamentation then becomes space-filling.

According to a general result (Tél 1990; Ott 1993) the deviation of the fractal dimension d of (any of) the manifolds from unity is the ratio of the reciprocal value of the average lifetime and the positive Lyapunov exponent λ of the chaotic advection in the leaked system. By using the estimate mentioned in the previous section, we obtain the relation $d \approx 2 + \ln(1 - \Delta)/\lambda$, where Δ is the area ratio of the leak, which is proportional in our case to $y_0 - y_c$.

Measuring the residence time, i.e., how long it takes for particles (initially homogeneously distributed in the whole flow) to leave the flow through the leaks, results in Fig. 4. In this figure, short residence times (dark blue regions) stand for locations where particles escape rapidly from the flow. Positions with long residence times (red colors) correspond to an approach towards one of the never-escaping orbits. Points with long residence times must therefore be close to the converging foliation, i.e., to the stable manifold (cf. Fig. 3a).

A surprising application of leaking a flow is in connection with the patterns traced out by reactions taking place in the same flow. Such patterns may appear due to strong concentration gradients in atmospheric chemistry, e.g., in ozone concentrations, or can be observed in ocean plankton dynamics. The basic mechanisms to generate them are the compression of the fluid elements

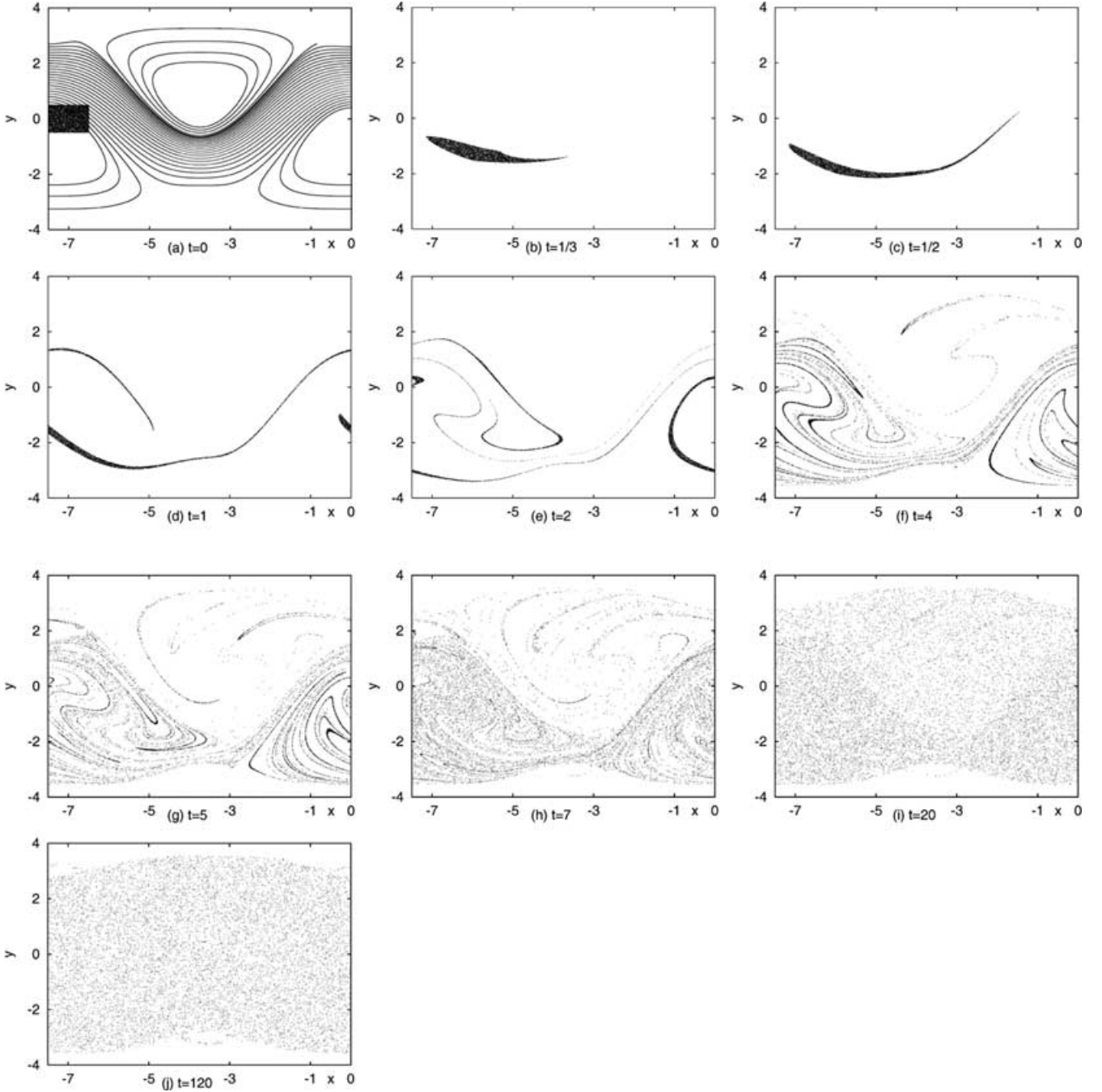


Fig. 2 Evolution of a droplet in the kinematic models (1)–(3) of a meandering jet. A droplet of dye, consisting of 10 000 particles uniformly distributed on the *black rectangle* shown in the first frame (a) evolves in time as shown in frames b ($t = 1/3$), c ($t = 3/4$), . . . j, ($t = 120$). The *upper left panel a*; ($t = 0$) also shows the streamlines of the unperturbed flow in the background. Stretching and folding characteristic for chaotic motion can be seen (e.g., e; ($t = 2$)). At some instant (e.g., f $t = 4$) the dye traces out a filamental structure which is smeared out after some more time. After $t = 120$ periods, all dye particles are distributed homogenously in the whole flow. Used parameters are: $\Psi_0 = 1$, $A_0 = 1.2$, $c = 0.12$, $\lambda = 1$, $k = 2\pi/7.5$, $\sigma = 0.3$, $\theta = \pi/2$, $\omega = 0.4$. Time is measured here and in all the following captions in units of the flow's period $2\pi/\omega$

towards the stable foliation of the flow, with the consequence of increasing local gradients, and the stretching of the fluid elements along the unstable filamentation of the flow. The concentration is then smoothed out along the unstable filamentation due to the experienced stretching (Hernández-García et al. 2002). Here, as an example, we will consider a biological reaction by superimposing a model of plankton dynamics on the two-dimensional meandering jet described above.

Particles are assumed again to be point-like. They are active, can react with each other, but do not modify the flow. In the examined model, the temporal evolution of the phytoplankton, its nutrient, and the zooplankton are

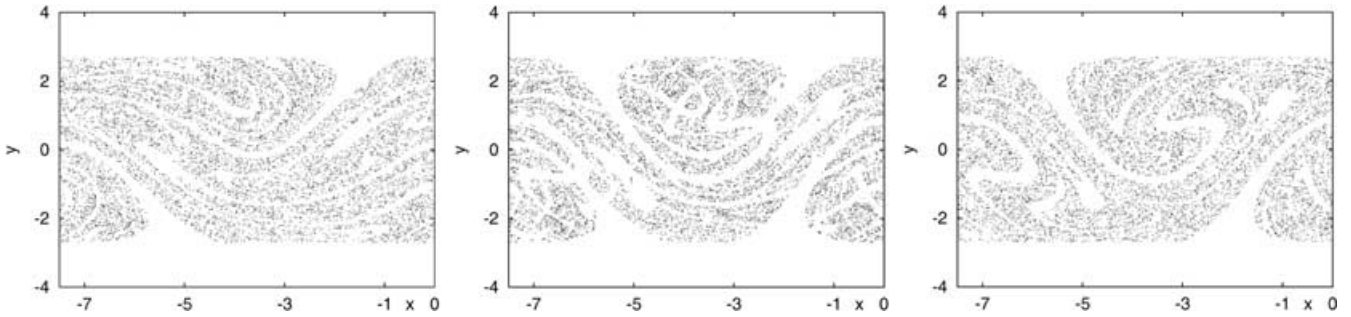


Fig. 3 Filamentary structures in the leaked flow (Eqs. 1–3) traced out by nonescaped particles after applying the analysis of Section 2. The *left panel* shows the converging filamentation, i.e., the stable manifold of the chaotic saddle: only those initial ($t = t_0 = 0$) positions out of an initially homogenous particle distribution ($N_0 = 50\,000$) on the region $[-7.5 : 0][-2.7 : 2.7]$ are plotted which do not escape during $\tau = 20$ periods. The *right panel* shows locations of the not yet escaped particles after $\tau = 20$ periods, which trace out the stretching filamentation, i.e., the unstable manifold of the chaotic saddle. The *panel in the middle* depicts the chaotic saddle itself, obtained from the points taken at $t = \tau/2$, and coincides with the intersection of its stable and unstable foliations

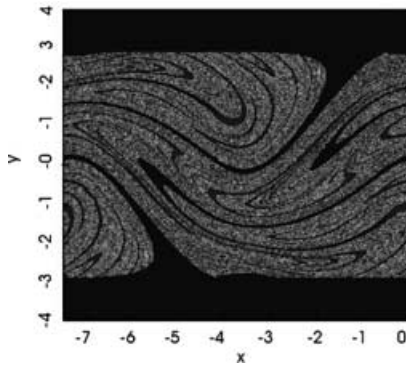


Fig. 4 Residence times. Particles starting from the *dark blue* regions need the shortest time to escape. *Light blue* denotes places where the residence times are within 4 and 7 periods. *Colors towards red* (residence time longer than 40, up to 99 periods) denote places with increasing residence times. $N_0 = 600\,800$ particles were used, initially distributed over a grid of mesh size $\delta = 0.01$ in the same region as in Fig. 3

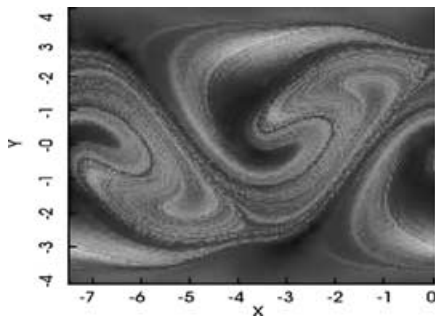


Fig. 5 Structures traced out by phytoplankton in a plankton model superimposed on the meandering jet. (Lopez et al. (2001)). Note the similarity with the stretching/unstable foliation shown in the right panel of Fig. 3

determined by advection–reaction–diffusion equations (see Lopez et al. 2001 for details). Nutrients are distributed in the flow and are eaten up by phytoplankton, which then grow in number. These biological reactions make complex filamentary structures appear, marked by different phytoplankton concentrations, shown in Fig. 5. Due to stretching, the concentration changes smoothly along the unstable foliation, but not so along the converging one. Therefore, directions corresponding to low concentration gradients trace out a part of the unstable foliation of the passive problem (cf. Fig. 5 with the right panel of Fig. 3). Since the backbone for an active process is, in general, the unstable filamentation of the passive dynamics (Toroczkai et al. 1998), it is not surprising that structures of the unstable manifold obtained by leaking the reaction free flow show striking similarities with those traced out by the active particles in the closed flow. Thus, by leaking a closed flow and studying the not yet escaped passive particles, we can mimic structures similar to those which appear in active processes. For a chemical model see Schneider et al. (2002).

3.2 A chaotically time-dependent flow

The temporal periodicity of the flow model used above seems to be a strong restriction. Flows changing quasiperiodically or chaotically in time, but characterized by smooth streamlines in space, form an interesting class of flows which has received recent attention. Since on snapshots taken with some sampling time, the velocity field appears to be a random (but not necessary weak) perturbation of the initial one, such flows are called random flows (Pierrehumbert 1994; Jacobs et al. 1997; Neufeld and Tél 1998). Two-dimensional random flows can be considered as elementary models of two-dimensional or geostrophic turbulence. A surprising feature of random flows is that tracer patterns generated by them are shown to exhibit – in spite of the randomness – clean fractal structures which can be described by the theory of random maps (Romeiras et al. 1990; Yu et al. 1991; Sommerer and Ott 1993).

To test how a random perturbation changes the stable and unstable filamentation in the meandering jet model, we modify the amplitude of the sinusoidal driving in Eq. (3) by adding a random shift to the average amplitude $\bar{\sigma}$ after each period $2\pi/\omega$ of time.

We thus take the streamfunction defined by Eqs. (1) and (3) with

$$\sigma = \bar{\sigma} + \delta\sigma_n, \quad (4)$$

where $\delta\sigma_n$ is a random number distributed uniformly in the range $[-0.05; 0.05]$ and kept constant over the n th period. The results obtained with the method of leaking are shown in Fig. 6. In spite of the fact that the random perturbation is not weak (its amplitude is one third of the average value $\bar{\sigma} = 0.3$), the filamentation remained clean. The actual shape of all the patterns is similar to what we see in the nonrandom case (Fig. 3), but minor details can be different (like, e.g., the precise form of the largest white tongues). Furthermore, all the patterns depend on the actual snapshot taken (see Fig. 6d,e,f) which is due to the fact that the flow is not periodic. (In the periodic case the location of the points of the nonescaped orbits is the same for $t = t_0$ and $t = t_0 + 1$, for $t = t_0 + \tau/2$ and $t = t_0 + \tau/2 + 1$, and for $t = t_0 + \tau$ and $t = t_0 + \tau - 1$.) The theory of random maps also implies (Jacobs et al. 1997; Neufeld and Tél 1998) that the fractal dimensions of the manifolds and the chaotic saddle do not depend on the snapshot taken. The similarity of the structures on subsequent snapshots indicates that the filamentation remains qualitatively the same as in a periodic flow. Thus, the method of leaking

the flow for visualizing its stable and unstable filamentation is applicable to random flows as well. Note that the shape of the stable foliation does not depend on the observed time span τ , but does depend on the instant (t_0) of the initialization of particles. The shape of the unstable foliation and the chaotic saddle both depend on τ and t_0 .

3.3 A dynamically consistent model with barriers

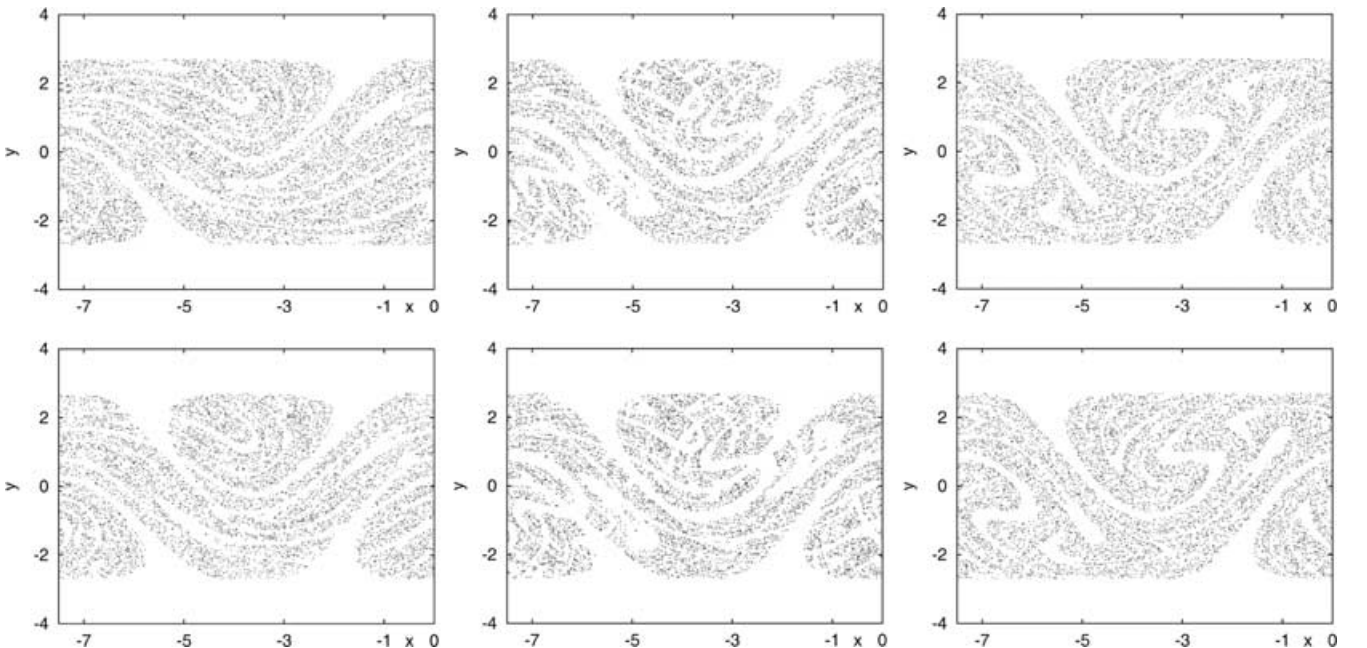
Instead of the kinematic model, we consider now a dynamically consistent (nonrandom) model of the jet derived by del Castillo-Negrete and Morrison (1993), which takes into account the conservation of potential vorticity in leading order. The flow is defined in a frame comoving with the slower wave of wavenumber k_2 by the stream-function:

$$\psi = -\tanh y + c_2 y + \epsilon_1 \cosh^{-2} y \cos(k_1 x - \Omega t) + \epsilon_2 \cosh^{-2} y \cos k, \quad (5)$$

where $\Omega = 2k_1/3\sqrt{1-3\beta/2}$ with β as the beta parameter, and $k_{1,2}^2 = 2(1 \pm \sqrt{1-3\beta/2})$, $c_2 = 1/3(1 - \sqrt{1-3\beta/2})$. With these parameters, the model exhibits bounded chaos interwoven with integrable regions (KAM-, Kolmogorov-Arnold-Moser“-tori).

The new feature of this flow is the appearance of a transport barrier around the jet which is a kind of coherent structure. Due to this barrier, there is no need to leak the flow on both sides, since there is in any case no communication between the lower and the upper part of the jet. Therefore, the filamentations are independent of each other in these two regimes. We apply an escape condition across the line $y = -y_c = -1.7$ only, and carry out the same procedure as in the first subsection in order to visualize the filamentation in the lower part. For

Fig. 6 Filamental structures in the random flow model of the meandering jet (Eqs. 1–4) opened up by leaking. The average driving amplitude is $\bar{\sigma} = 0.3$, as in Fig. 3, but there is a random variance around it of half-width 0.05 (see Eq. 4). The *panels* show the points of the orbits not escaping over $\tau = 20$ periods at times $t = 0$, $t = 10$, $t = 20$ and $t = 1$, $t = 11$, $t = 19$. The *left*, *middle*, and *right columns* correspond to the stable foliation, the chaotic saddle, and the unstable foliation, respectively. Note that the *plots above each other* are not the same due to the aperiodic time dependence of the flow. Initial conditions (apart from the number of particles started: $N_0 = 100\,000$) and leak are as in Fig. 3



simplicity, we show only the endpoints of the non-escaped orbits in Fig. 7, corresponding to the unstable foliation. The pattern seen is somewhat different from the previous cases because of the central barrier. Note that the visualized structures of the eddies correspond to the spirals that Yuan et al. (2002) found in their patchiness plots. Now we can see that these structures (unstable manifold) are indeed created by the underlying motion, composed of the rotation in the eddies, and of the motion of the comoving frame.

The leaking method proposed here for visualizing structures in the flow is applicable for all parameter ranges and implies also an applicability in three-dimensional systems.

4 Discussion

The method proposed here is based on the following tracer trajectories. The models used were chosen to be

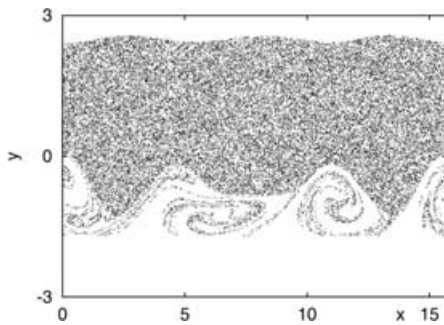
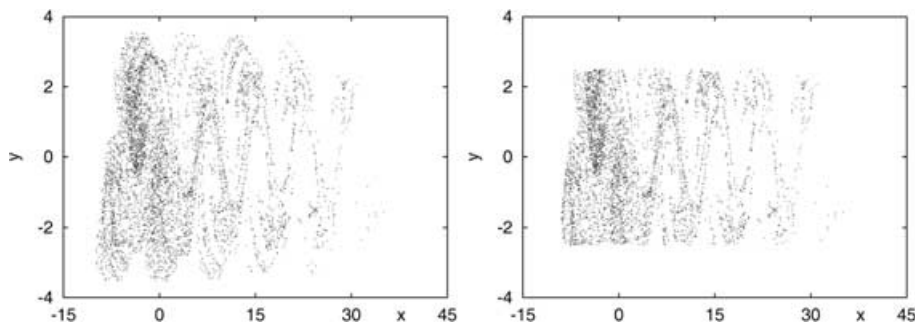


Fig. 7 Filamentation in the dynamically consistent model (Eq. 5) of the jet. The endpoints of orbits which do not cross the line $y = -1.7$ over a time period of $3 \times 2\pi/\Omega$ trace out the unstable filamentation below the centerline of the jet. The leaking of the system affects only the lower part of the jet due to the transport barrier in the middle; no structures become visible in the middle and upper parts. The initial condition was a uniform distribution of $N_0 = 50\,000$ particles in the slab $-1.7 \leq y \leq 2.5$ over the spatial period $3 \times 2\pi/k_2$. Parameters: $\varepsilon_1 = 0.1$, $\varepsilon_2 = 0.3$, $\beta = 0.614$ ($k_1 = 1.6$, $k_2 = 1.2$, $c_2 = 0.24$, $\Omega = 0.3$)

Fig. 8 *Left panel:* Spaghetti diagram. Time-continuous trajectories of $N_0 = 1200$ tracers in models (1)–(3), started homogeneously distributed in the region $[-7.5 : 0][-2.5 : 2.5]$, depicted over a time interval of $\tau =$ five periods. *Right panel:* Same as left panel, but now only plotting trajectories staying in the leaked region $|y| \leq 2.5$ over five time units. The kinematic model is taken with the same parameters as in Figs. 2–5



close to realistic flows in the oceans or atmosphere. In particular, parameters are taken to roughly correspond to those of the Gulf Stream. Our method can thus be applied to oceanic flows in which the motion of floats is monitored over a long period of time: by selecting a region of observation smaller than the full region accessible to the tracers, and keeping only those trajectories which stay within this region over a long period, the spaghetti diagrams (Fig. 8) are cleaned and a filamentation appears by plotting the initial and the final positions of the not yet escaped tracers. The basic limitation in practice is set by the number of tracers used. We carried out simulations to check what the smallest number of tracers is at which the first signs of filamentation optically appear. In our first model, this number was found to be on the order of 1200 (see Fig. 9). There is therefore hope for applying this method to visualizing Lagrangian patterns in the ocean if the number of tracers available grows on the order of 1000. The visibility of the structures depends somewhat on the initial particle distribution (see Fig. 9, right panel).

Next, we compare our method with another 1 aiming to determine the so-called finite time or effective manifolds (Miller et al. 1997; Haller and Poje 1998; Haller and Yuan 2000; Sandstede et al. 2000; Kuznetsov et al. 2002; Poje et al. 2002; Jones and Winkler (in press); Yuan et al. 2002). The latter can be applied to any aperiodic flow, also to flows which become stationary after some time. The purpose is to identify the analogues of saddle (hyperbolic) points in these flows and, after finding some of them, to determine a finite segment of their stable and unstable manifolds. In the knowledge of these, the lobe dynamics (Beigie et al. 1990; Rom-Kedar et al. 1990; Wiggins 1992) can be applied to quantify fluid transport over a finite period of time. The applicability of our method, in contrast, requires that the flow does not change its basic character over a longer period of time (it does not die out), although its temporal behavior can also be chaotic. What we gain by the existence of such a fluid dynamical “steady state” is the applicability of the theory of chaotic systems, which implies that not only a few, but a large number (an infinite number in principle) of hyperbolic never-escaping orbits can be present. All the midpoints (taken at time $t = t_0 + \tau/2$) are of this type, and form the chaotic saddle of the leaked flow. The fractal foliations related to times t_0 and $t_0 + \tau$ can be considered as stable and

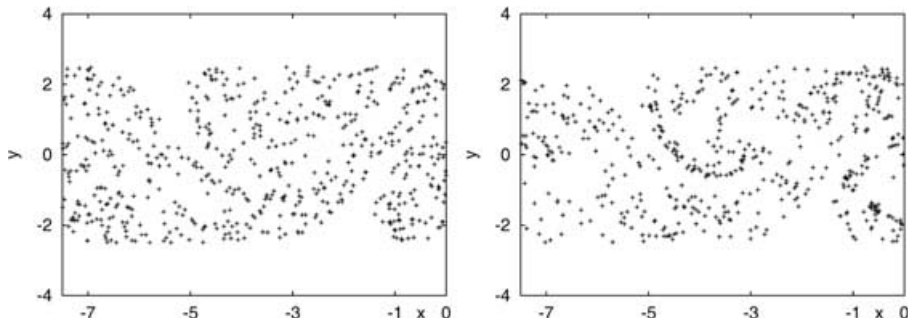


Fig. 9 Unstable filamentation traced out by a “small” ensemble. *Left panel* Same data is used as in Fig. 8 (same τ, N_0 , and initial distribution) but represented according to the leaking method described in the main text. Only the endpoints of trajectories at $\tau = 5$ have been plotted. Trajectories which go further than $y = \pm 2.5$ are not depicted. Endpoints are plotted over the basic wavelength $L = 7.5$ of the stream after applying periodic boundary conditions in x . *Right panel* As left panel, but now the particles were initially distributed in a stripe at $-0.5 \leq y \leq 0.5$ over one wavelength ($-7.5 \leq x \leq 0$)

unstable manifolds, respectively; however, they do not belong to a few isolated fixed points, but to the full chaotic set. Thus, we obtain a better characterization of the main transport/stretching directions of the system, and by means of a much simpler and faster method than needed by the one reconstructing the finite time manifolds of only a few hyperbolic points. Our method thus always provides a fractal foliation. In cases of decaying fluid activity, it cannot be applied, and then the effective manifolds are necessarily nonfractal objects.

In conclusion, by leaking, i.e., by cutting out a finite region of a closed chaotic flow, and thus making an escape of particles possible, we can visualize fractal filamental patterns out of a formerly homogenous tracer distribution. As pointed out, by visualizing the unstable manifold, we are also able to reconstruct or mimic structures which will be traced out by active processes, e.g., by phytoplankton or pollutants in the flow.

Acknowledgements Useful discussions are acknowledged with A. Bracco, U. Feudel, E. Hernández-García, Z. Neufeld, O. Piro, A. Provenzale, J. Schmalzl, and J. Weiss. We are grateful to the authors of López et al. (2001), who kindly allowed us to use one of their figures. This research has been supported by the Hungarian Research Foundation (OTKA T032423). J.S. is grateful for a scholarship from the International Max Planck Research School for Biomimetic Systems (IMPRS). J.S. and T.T. were supported by the DAAD 324/PPP-Ungarn-ssch grant.

References

- Alperin MJ, Suayah IB, Benninger LK, Martens CS (2002) Modern organic carbon burial fluxes, recent sedimentation rates, and particle mixing rates from the upper continental slope near Cape Hatteras, North Carolina (USA). *Deep-Sea Res II* 49: 4645–4665
- Alvarez MM, Muzzio FJ, Cerbelli S, Adrover A, Giona M (1998) Self-similar spatiotemporal structure of intermaterial boundaries in chaotic flows. *Phys Rev Lett* 81: 3395–3398
- Beigie D, Leonard A, Wiggins S (1990) Invariant manifold templates for chaotic advection. *Chaos, Solitons Fractals* 4: 749–868
- Bower A (1991) A simple kinematic mechanism for mixing fluid parcels across a meandering jet. *J Phys Oceanogr* 21: 173–180
- Cencini M, Lacorata G, Vulpiani A, Zambianchi E (1999) Mixing in a meandering jet: a Markovian approximation. *J Phys Oceanogr* 29: 2578–2594
- de Fatima M, Gabardo IT, Carneiro MER, Barbanti SM, da Silva GC, Massone CG (2002) Brazilian oil spills chemical characterization – Case Studies. *Environmental Forensics* 3: 303–321
- del Castillo-Negrete D, Morrison PJ (1993) Chaotic transport by Rossby waves in shear flow. *Phys Fluids (A)* 5: 948–965
- Dutkiewicz S, Paldor N (1994) On the mixing enhancement in the meandering jet due to the interaction with an eddy. *J Phys Oceanogr* 24: 2418–243
- Farmer D, Pawlowicz R, Jiang R (2002) Tilting separation flows: a mechanism for intense vertical mixing in the coastal ocean. *Dynam Atmos Oceans* 36: 43–58
- Flagg CN, Pietrafesa LJ, Weatherly GL (2002) Springtime hydrography of the southern Middle Atlantic Bight and the onset of seasonal stratification. *Deep-Sea Res (II)* 49: 4297–4329
- Giona M, Adrover A, Muzzio F, Cerbelli S (1999) The geometry of mixing in time-periodic chaotic flows. Asymptotic directionality in physically realizable flows and global invariant properties. *Physica (D)* 132: 298–324
- Haller G, Poje AC (1998) Finite time transport in aperiodic flows. *Physica (D)* 119: 352–380
- Haller G, Yuan G (2002) Lagrangian coherent structures and mixing in two-dimensional turbulence. *Physica (D)* 147: 352–370
- Hernández-García E, López C, Neufeld Z (2002) Small-scale structure of nonlinearly interacting species advected by chaotic flows. *Chaos* 12: 470–478
- Huppert A, Stone L (1998) Chaos in the Pacific coral reef bleaching cycle. *Am Natural* 152: 447–459
- Jacobs J, Ott E, Antonsen T, Yorke J (1997) Modeling fractal entrainment sets of tracers advected by chaotic temporally irregular fluid flows using random maps. *Physica (D)* 110: 1–17
- Jones CKRT, Winkler S Do invariant manifolds hold water? In: Fiedler B, Iooss G, Koppell N (eds) *Handbook of dynamical systems III: towards applications*. (In press)
- Knobloch E, Weiss JB (1987) Chaotic advection by modulated traveling waves. *Phys Rev (A)* 36: 1522–1524
- Kuznetsov L, Toner M, Kirwan Jr. Ad, Jones CKRT, Kantha LH, Choi J (2002) The loop current and adjacent rings delineated by Lagrangian analysis of the new-surface flow. *J Mar Res* 60: 405–429
- Lai Y-C, Tél T, Grebogi C (1993) Stabilizing chaotic-scattering trajectories using control. *Phys Rev* 48: 709–717
- López C, Neufeld Z, Hernández-García E, Haynes PH (2001) Chaotic advection of reacting substances: plankton dynamics on a meandering jet. *Phys Chem Earth (B)* 26: 313–317
- Miller PD, Jones CKRT, Rogerson AM, Pratt LJ (1997) Quantifying transport in numerically generated velocity fields. *Physica (D)* 110: 105–122
- Neufeld Z, Tél T (1998) Advection in chaotically time-dependent open flows. *Phys Rev (E)* 57: 2832–2842

- Ott E (1993) *Chaos in dynamical systems*. Cambridge University Press, Cambridge
- Ottino JM (1989) *The kinematics of mixing: stretching, chaos and transport*. Cambridge University Press, Cambridge
- Perugini D, Poli G, Gatta GD (2002) Analysis and simulation of magma mixing processes in 3D. *Lithos* 65: 313–330
- Pierrehumbert R (1994) Tracer microstructure in the large-eddy-dominated regime. *Chaos Solitons Fractals* 4: 1091–1110
- Poje AC, Toner M, Kirwan, Jr. AD, Jones CKRT (2002) Drifter launch strategies based on Lagrangian templates. *J Phys Oceanogr* 32: 1855–1869
- Rogerson AM, Miller PD, Pratt LJ, Jones CKRT (1999) Lagrangian motion and fluid exchange in a barotropic meandering jet. *J Phys Oceanogr* 29: 2635–2655
- Romeiras E, Grebogi C, Ott E (1990) Multifractal properties of snapshot attractors of random maps. *Phys Rev (A)* 41: 784–799
- Rom-Kedar V, Leonard A, Wiggins S (1990) An analytical study of transport, mixing and chaos in an unsteady vortical flow. *J Fluid Mech* 214: 347–394
- Rothstein D, Henry E, Gollub JP (1999) Persistent patterns in transient chaotic fluid mixing. *Nature* 401: 770–772
- Samelson RM (1992) Fluid exchange across a meandering jet. *J Phys Oceanogr* 22: 431–440
- Sandstede B, Balasuriya S, Jones CKRT, Miller P (2000) Melnikov theory for finite-time vector fields. *Nonlinearity* 13: 1357–1377
- Schneider J, Tél T, Neufeld Z (2002) Dynamics of “leaking” Hamiltonian systems. *Phys Rev (E)* 66: 066218
- Sommerer JC, Ott E (1993) Particles floating on a moving fluid: a dynamically comprehensive physical fractal. *Science* 259: 335–339
- Tél T (1990) Transient chaos. In: Lin H-B (ed) *Directions in chaos*. World Scientific, Singapore, pp 149
- Toroczkai Z, Tél T (eds). (2002) Focus issue on active chaotic flow. *Chaos* 12: 372–530
- Toroczkai Z, Károlyi G, Péntek A, Tél T, Grebogi C (1998) Advection of active particles in open chaotic flows. *Phys Rev Lett* 80: 500–503
- Voth GA, Haller G, Gollub JP (2002) Experimental measurements of stretching fields in fluid mixing. *Phys Rev Lett* 88: 254501
- Wiggins S (1992) *Chaotic transport in dynamical systems*. Springer, Berlin Heidelberg, New York
- Yu L, Ott E, Chen Q (1991) Fractal distribution of floaters on a fluid surface and the transition to chaos for random maps. *Physica (D)* 53: 102–124
- Yuan G-C, Pratt LJ, Jones CKRT (2002) Barrier destruction and Lagrangian predictability at depth in a meandering jet. *Dyna Atmosph Oceans* 35: 41–61